GPU Acceleration of the Material Point Method

Fabian Meyer

University of Koblenz

Kolloquium Computergrafik, 14 February 2019

A Brief MPM Overview: Do You Want to Build a Snowman?

A short historical summary of MPM:

- Belongs to family of particle-in-cell(PIC) techniques [EHB57].
- Initial application to solids [SZS95] $\rightarrow$ MPM
- From research to production in *Disney's* animation film *Frozen* [Sto+13].
- Avalanche research [Gau+18]

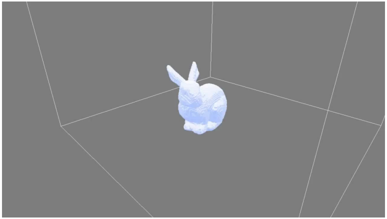

Video result of my bachelor thesis on the simulation of snow [Mey15].

PIC ideas:

- Combine Lagrangian particles & Eulerian grid
- Particles store all information

Typical PIC/MPM roundtrip:

1. Particle-to-grid(P2G) transfer to an unmoving grid
2. Solve discretized governing equations on grid
3. Grid-to-particle(G2P) transfer back to particles & move them

$\Rightarrow$ **meshfree, non-empirical**

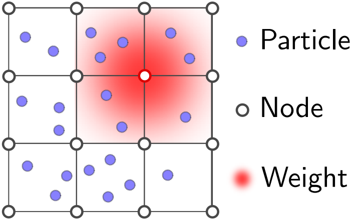

Transfers: Interpolation functions are defined over grid nodes.

GPGPU for performance enthusiasts

Why would('nt) you?

Drawbacks:

- Interactivity much easier on CPU, but slow PCI-Bus communication
- Code is mostly written against GPU architecture
- A lot of strain on the programmer

Benefits:

- Data is already on the GPU for rendering
- **Higher parallelization acceleration**

Governing Equations: Conservation of Mass & Momentum

Conservation of mass, continuum assumption holds.
Lagrangian (moving with a particle ${}_0\boldsymbol{x}$):

$$ {}_0^tJ\rho({}_0\boldsymbol{x}, t) = \rho({}_0\boldsymbol{x}, 0). \tag{1} $$

Eulerian (outside observer ${}_t\boldsymbol{x}$):

$$ \frac{\partial}{\partial t}\rho({}_t\boldsymbol{x}, t) = -\vec{\nabla} \cdot (\rho({}_t\boldsymbol{x}, t)\boldsymbol{v}({}_t\boldsymbol{x}, t)). \tag{2} $$

Lagrangian and Eulerian view measure differently but give same results. Equations are given in the strong form! [Jia+16][Abe12]

Conservation of momentum:
Lagrangian (moving with a particle ${}_0\boldsymbol{x}$):

$$\rho({}_0\boldsymbol{x}, 0)\boldsymbol{a}({}_0\boldsymbol{x}, t) = \vec{\nabla} \cdot \boldsymbol{P}({}_0\boldsymbol{x}, t) + \boldsymbol{f}^{\text{body}}({}_0\boldsymbol{x}, t){}_0^t J. \qquad (3)$$

Eulerian (outside observer ${}_t\boldsymbol{x}$):

$$\rho({}_t\boldsymbol{x}, t)\boldsymbol{a}({}_t\boldsymbol{x}, t) = \vec{\nabla} \cdot \boldsymbol{\sigma}({}_t\boldsymbol{x}, t) + \boldsymbol{f}^{\text{body}}({}_t\boldsymbol{x}, t) \qquad (4)$$

Solving this equation will tell us how the velocity fields $\boldsymbol{v}({}_t\boldsymbol{x}), \boldsymbol{v}({}_0\boldsymbol{x})$ change on the whole domain due to acceleration $\boldsymbol{a}$. This is important to advect particles accounting for all forces. [Jia+16][Abe12]

The Pretty Strong but Mathematically Weak Formulation

Weak Formulation (or Principle of Virtual Work):
Dot product equations with arbitrarily 'test functions' $\boldsymbol{q}$ and apply divergence theorem:

$$\int_{\Omega^0} {}_0\boldsymbol{q} \cdot \left[({}_0\rho_0)({}_0\boldsymbol{a}) - {}_0\boldsymbol{f}^{\text{body}}\,{}_0^tJ \right] d_0\boldsymbol{x} = \int_{\partial\Omega^{t^n}} {}_t\boldsymbol{q} \cdot \boldsymbol{\sigma}\, d_t\boldsymbol{A} - \int_{\Omega^{t^n}} \nabla_t \boldsymbol{q} : \boldsymbol{\sigma}\, d_t\boldsymbol{x}. \tag{5}$$

A strong solution is also a solution to the weak formulation. Leave out body forces(like gravity) and boundary condition (e.g. collisions) for now:

$$\int_{\Omega^0} {}_0\boldsymbol{q} \cdot ({}_0\rho_0)({}_0\boldsymbol{a}) d_0\boldsymbol{x} = \int_{\Omega^{t^n}} \nabla_t \boldsymbol{q} : \boldsymbol{\sigma}\, d_t\boldsymbol{x}. \tag{6}$$

Weak Derivative:

$y = |t|$ has weak derivative:

$$v = \begin{cases} -1, & \text{if } t < 0 \\ c, & \text{if } t = 0 \\ 1, & \text{if } t > 0 \end{cases}$$

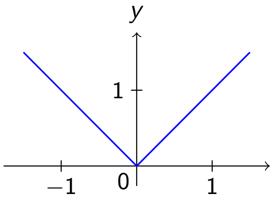

Heaviside step function has no weak derivate:

$$s = \begin{cases} 0, & \text{if } t < 0 \\ 1, & \text{if } t \geq 0 \end{cases}$$

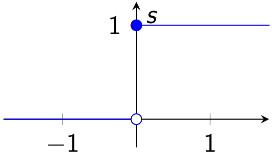

Allows for point loads, material discontinuities and more. [Bat06]

Discretization of Space and Time

Time discretization with implicit midpoint scheme:

$$\frac{y^{n+1} - y^n}{\Delta t} = f^{n+\frac{1}{2}} = f\left(t^n + \frac{\Delta t}{2}, \frac{1}{2}y^n + \frac{1}{2}y^{n+1}\right) \qquad (7)$$

- **implicit** requires linear system solve $\Rightarrow$ more stable, larger time steps
- **midpoint** as it conserves gov. equations

$$\Rightarrow \int_{\Omega^t} {}_t\boldsymbol{q} \cdot {}_t\rho({}_t\boldsymbol{v}^{n+1} - {}_t\boldsymbol{v}^n) d_t\boldsymbol{x} = \int_{\Omega^{t^n}} \nabla_t \boldsymbol{q} : \boldsymbol{\sigma}^{n+\frac{1}{2}} d_t\boldsymbol{x}. \qquad (8)$$

Space Discretization is done in a Galerkin/FEM fashion with grid based interpolants w_i with limited support. Here dyadic products

$$w_i(\boldsymbol{x}) = w(\boldsymbol{x} - \boldsymbol{x}_i) = w(\frac{1}{h}(x - x_i))w(\frac{1}{h}(y - y_i)w(\frac{1}{h}(z - z_i)) \quad (9)$$

of cubic b-splines suffice:

$$w(x) = \begin{cases} \frac{1}{2}|x|^3 - |x|^2 + \frac{2}{3} & 0 \leqslant |x| < 1 \\ \frac{1}{6}(2 - |x|)^3 & 1 \leqslant |x| < 2 \\ 0 & 2 \leqslant |x| \end{cases} . \quad (10)$$

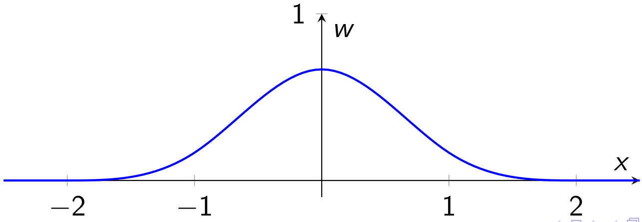

Thus set in:

$$
{}_t\boldsymbol{q}(\boldsymbol{x}, t^n) = \sum_i \boldsymbol{e}_i w_i(\boldsymbol{x}), {}_t\boldsymbol{v}^{n(+1)}(\boldsymbol{x}) = \sum_j \boldsymbol{v}_j^{n(+1)} w_j(\boldsymbol{x}).
$$

Combine it with numerical integration where the particles function as quadrature points [SKB08]:

$$
\begin{aligned}
g_i &= \int_\Omega g(\boldsymbol{x}) w_i(\boldsymbol{x}) d\boldsymbol{x} \\
&\approx \sum_p g_p w_i(\boldsymbol{x}_p) V_p. \qquad (11)
\end{aligned}
$$

due to integration by midpoint rule:

$$
\int_\Omega f(x)dx \approx \sum_{i=1}^{N} f(x_i)\, h_i. \qquad (12)
$$

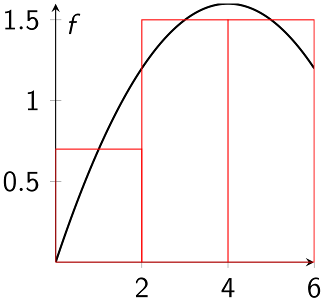

Velocity Fields: APIC-Transfers

PIC-transfer

1. $(m\boldsymbol{v})_i^n = \sum_p w_{ip}^n m_p \boldsymbol{v}_p^n$
2. $\boldsymbol{v}_i^n = \frac{(m\boldsymbol{v})_i^n}{m_i^n}$
3. $\boldsymbol{v}_{p,PIC}^{n+1} = \sum_i w_{ip}^n \boldsymbol{v}_i^{n+1}$

APIC-transfers add a local velocity field $\boldsymbol{C}_p^n$ around $\boldsymbol{v}_p^n$:

$$(m\boldsymbol{v})_i^n = \sum_p w_{ip}^n m_p \left(\boldsymbol{v}_p^n + \boldsymbol{C}_p^n(\boldsymbol{x}_i^n - \boldsymbol{x}_p^n)\right)$$

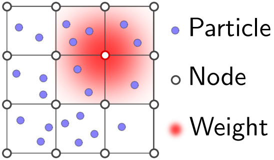

P2G-transfer $\sum_p$

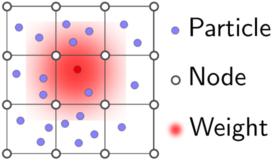

G2P-transfer $\sum_i$

Layout of the data: SoA vs. AoS

Coalescing:

SoA-Layout

```
struct Container{
  vec4 positions[n];
  vec4 velocities[n];
} Particles;
```

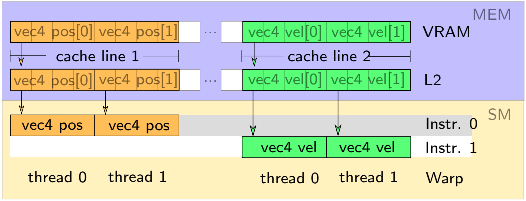

Structures of arrays(SoA)

AoS-Layout

```
struct Particle {
  vec4 position;
  vec4 velocity;
} Particles[n];
```

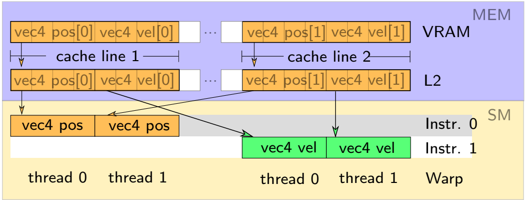

Arrays of structures(AoS)

Nvidia Nsight[NVI] now offers metrics to identify bottlenecks:

Metric	**Description**
VRAM SOL%	memory througput w.r.t. to hardware limit
SM SOL%	instruction throughput
L2 SOL%	L2-cache throughput
Tex SOL%	L1-cache throughput
SM Issue Util.%	amount of cycles an instr. was issued

A simple map(`y=length(x)`) shader on 1024×1024 Elements SoA vs. AoS differences:

Layout	$\Delta t_c(\mu s)$	Speedup	VRAM	SM	L2	SM Issue Util.
AoS(1 instr.)	243	-	77.7%	7.3%	30.3%	6.8%
SoA(1 instr.)	**120**	2.26x	75.4%	**14.3%**	29.4%	**14.0%**
AoS(2 instr.)	275	-	61.3%	**41.8%**	**53.8%**	48.9%
SoA(2 instr.)	240	1.16x	75.4%	29.4%	20.0%	62.3%

⇒ SoA increases coalescing for non-random access.

Parallel Reduction & Scan

Assuming an associative `binary_op(x,y):=` $x \circ y$, a neutral element e of the `binary_op`, and an array of values $[a_0, a_1, ..., a_n]$.

- **Parallel reduction** computes the value:

$$r = a_0 \circ a_1 \circ ... \circ a_n. \tag{13}$$

- (Exclusive) **scan** computes the array:

$$[e, a_0, (a_0 \circ a_1), (a_0 \circ a_1 \circ a_2), \ ... \ , (a_0 \circ a_1 \circ a_2 \circ ... \circ a_{n-1})]. \tag{14}$$

Here, only shared memory approaches without (NVIDIA exclusive) warp shuffle operations.

Shared Memory Bank Conflicts:

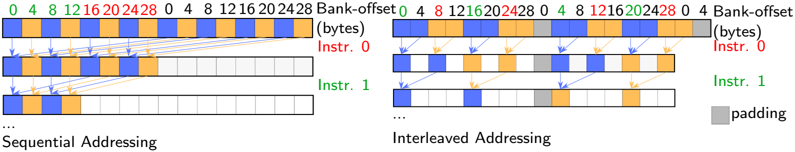

Interleaved addressing causes bank conflicts (Short Scoreboard activity) $\Rightarrow$ padding needed.

Method	Δt_c	Speedup	VRAM	SM	Sel. Warp-Stall Reas.
Interl. no padd.	305	-	23.0%	**60.9%**	S. Scoreb.(17.2%)
Sequential	141	2.16x	**49.8%**	37.1%	**S. Scoreb.(2.0%)**

Table: Parallel reduction on 1024×1024 vectors with `y=length(x)` as input.

More elements than thread group size require pyramid schemes.

Sequential work: multiple elements per thread.

- Memory latency hiding (Long Scoreboard up)
- Higher reduction factor each dispatch $\Rightarrow$ Less global memory indirections
- Unrolling loops can help but adds register pressure.

Method	Δt_c	Speedup	VRAM	SM	Sel. Warp-Stall Reas.
Sequential	141	2.16x	49.8%	37.1%	S. Scoreb.(2.0%)
Seq. (2x)	100	3.05x	69.5%	26.2%	L. Scoreb.(80.1%)
Seq. (128x)	98	3.1x	**72.9%**	16.9%	**L. Scoreb.(84.4%)**
Seq. (256x)	101	3.0x	66.4%	14.6%	L. Scoreb.(76.9%)

Table: Parallel reduction on 1024×1024 vectors with `y=length(x)` as input. Methods have 504, 8, 4 thread groups, respectively. A GTX970 has 13 SMs.

Scan is similar but cannot profit as much from sequential work having to keep multiple elements in register memory.

Binning & Counting Sort: Where Are You?

Grid node does not know its neighboring particles ⇒ Binning.

Binning combines nicely with **Counting Sort:**

1. **Binning**: Per node counting.
2. **Scan**: Computes new memory offset for particles.
3. **Reordering**: Give back indexing list or do deep copy.

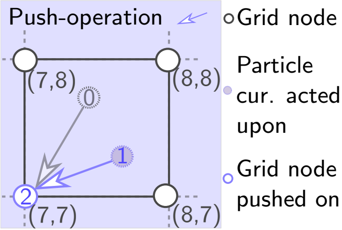

Sorting can dramatically increase workload performance of subsequent steps for neighboring queries:

1. Deep sorted accesses are now **coalesced**.
2. **Data reuse** due to L2-Cache and/or shared memory.

Double buffer particles to use last sorted state as input for new sorting to profit from item 1 and 2!

Ordering	$\Delta t_c(\mu s)$	Speedup	VRAM	SM	L2	L2-Hit
Random	1,516	-	25.0%	3.4%	9.1%	10.8%
Deep sorted	218	6.95x	**75.3%**	24.4%	**35.0%**	**37.8%**

Table: Order dependency of binning of 1024×1024 randomly positioned particles in a $128 \times 128 \times 128$ grid.

The MPM Specific Transfers

All MPM operations belong to one of those parallelization schemes:

- 1 thread : 1 particle: $\square_p = \square_p \circ \square_p \circ \ldots \circ \square_p$.
- 1 thread : 1 node: $\square_p = \square_p \circ \square_p \circ \ldots \circ \square_p$.
- P2G-transfer: $\square_i = \sum_p \square_p \circ \square_{ip}$.
- G2P-transfer: $\square_p = \sum_i \square_i \circ \square_{ip}$.

MPM-Transfers are executed **multiple times per physical frame** with varying numbers of variables and mathematical operations.

$\Rightarrow$ Preprocessing steps only need to be done **once per physical frame**. Sorting already introduced as one of these.

hi

1. [Jia+16]

Rohan Abeyaratne. *Volume II of Lecture Notes on,The Mechanics of Elastic Solids: Continuum Mechanics*. http://web.mit.edu/abeyaratne/Volumes/RCA_Vol_II.pdf. [Online; accessed 08-November-2018]. MIT Department of Mechanical Engineering, 2012.

Klaus-Jürgen Bathe. *Finite element procedures*. Klaus-Jurgen Bathe, 2006.

Martha W Evans, Francis H Harlow, and Eleazer Bromberg. *The particle-in-cell method for hydrodynamic calculations*. Tech. rep. LOS ALAMOS NATIONAL LAB NM, 1957.

Johan Gaume et al. "Unified modeling of the release and flow of snow avalanches using the Material Point Method". In: Aug. 2018.

Chenfanfu Jiang et al. "The material point method for simulating continuum materials". In: *ACM SIGGRAPH 2016 Courses*. ACM. 2016, p. 24.

Fabian Meyer. "Simulation von Schnee". Bachelor's Thesis. Universität Koblenz-Landau, Institut für Computervisualistik, 2015.

NVIDIA Corporation. *NVIDIA Nsight*. https://docs.nvidia.com/nsight-visual-studio-edition/Content/Performance_Markers_OGL.htm. [Online; accessed 5-December-2018].

Michael Steffen, Robert M Kirby, and Martin Berzins. "Analysis and reduction of quadrature errors in the material point method (MPM)". In: *International journal for numerical methods in engineering* 76.6 (2008), pp. 922–948.

Alexey Stomakhin et al. "A material point method for snow simulation". In: *ACM Transactions on Graphics (TOG)* 32.4 (2013), p. 102.

Deborah Sulsky, Shi-Jian Zhou, and Howard L Schreyer. "Application of a particle-in-cell method to solid mechanics". In: *Computer physics communications* 87.1-2 (1995), pp. 236–252.